EFFECT OF Nb AND Zn ELEMENT DOPING ON BARIUM STRONTIUM COBALT FERRITE-BASED CATHODE FOR SOLID OXIDE FUEL CELL – A SHORT REVIEW

Umira Asyikin Yusop, Nurul Farhana Abd Rahman, Yohannes Nyambong Anak Lowrance, Zolhafizi Jaidi, Mohd Faizal Tukimon, Mohd Azham Azmi, Azzura Ismail, Shahruddin Mahzan and Hamimah Abd Rahman*

Department of Manufacturing Engineering, Faculty of Mechanical and Manufacturing Engineering, Universiti Tun Hussein Onn Malaysia, 86400 Parit Raja, Batu Pahat, Malaysia.

*hamimah@uthm.edu.my

Abstract. Alternative energy sources are needed to meet global energy demands, and a dependable solid oxide fuel cell (SOFC) has demonstrated system reliability. The commercialization of SOFC, especially for intermediate to low-temperature applications, can be widely achieved after meeting a few system requirements and locating suitable material candidates. Therefore, this review is conducted to observe the current approach to the material development for intermediate temperature SOFC (IT-SOFC) and the influence of doping the element on BSCF-based cathode properties. This article reviewed two types of doping elements, namely, Niobium (Nb) and Zinc (Zn), and their chemical, physical, thermal and electrochemical characteristics. The dopant material was substituted in the B-site of BSCF cathode material to increase the cell performance. As observed from the study, it greatly enhanced the performance and chemical stability of BSCF as a cathode material. Interestingly, Nb-doping increased the chemical stability and CO_2 tolerance of BSCF-based materials under high oxidation conditions, while Zn doping improved the electrocatalytic activity of the oxygen reduction (ORR) process. This review found that BSCF perovskite is an attractive and promising candidate material for SOFC. Still, the compatibility of the cathode material in terms of chemical, physical, thermal and electrochemical properties should be further investigated to achieve optimum parameters for outstanding cell performance.

Keywords: BSCF-based cathode, doping, IT-SOFC, niobium, zinc

Article Info

Received 15th December 2021
Accepted 19th March 2022
Published 20th April 2022

ISSN: 1823-7010, eISSN: 2600-7444

Introduction

Global energy consumption necessitates the development of alternative power sources that can benefit the world in various ways [1]. A dependable fuel cell is an electrochemical system that can convert energy from chemical into electrical [2] in a clean and environmentally friendly manner [3-4] with minimal pollution [5]. Among all fuel cell types, the solid oxide fuel cell (SOFC) has demonstrated guaranteeing performance suitable for today's concerns [6-7] also a promising clean and efficient power generation device [8]. However, SOFC has a major operating temperature issue [9] because it typically operates at a high temperature of approximately 1000 °C [1]. The operation of SOFC at temperatures ranging from 700 °C to 900 °C might have an adverse effect on the system's overall efficiency [10].

The required operating temperature makes commercialization impossible for SOFC because it limits the use of substances and increases the process's cost [10]. This issue can be avoided by reducing the operating temperature to a moderate level at 600 °C to 800 °C [11]. SOFCs are attractive candidates for future technology inventions for converting energy, and considerable work has already been expended on reducing their working temperature for broader usage [10, 12]. This reduction can provide numerous benefits to the operation, including reduced material degradation, increased material structure stability, longer service life, and reduced processing costs [6-10, 13]. However, as a cathode material selection, lower temperatures could reduce cathode catalytic performance for the oxygen reduction reaction (ORR) process and thus decrease the electrochemical performance of intermediate SOFC (IT-SOFC) [14-15]. Hence, the appropriate cathode materials for IT-SOFC should be investigated. The exploration of high-potential cathode materials needs to consider two factors: high catalytic activity and improved chemical stability [11, 13].

Several investigations were conducted to produce better cathode material compounds and optimize their microstructure to improve the catalytic properties for the ORR process in IT-SOFC. Among various cathode substances investigated, perovskite oxides material with mixed oxygen ionic and electronic conductivity (MIEC) has received the highest attention [16]. In the last few years, alternative materials for cathode composites like $La_{0.6}Sr_{0.4}Co_{0.2}Fe_{0.8}O_{3-\delta}$ (LSCF), $Ba_{0.5}Sr_{0.5}Co_{0.8}Fe_{0.2}O_{3-\delta}$ (BSCF), $BaCo_{0.4}Fe_{0.1}Y_{0.1}O_{3-\delta}$ (BSCFY0.1), $LaBa_{0.5}Sr_{0.5}Fe_2O_{6-\delta}$ (LBSF) and $PrBa_{0.5}Sr_{0.5}Co_{2-x}Fe_xO_{5+\delta}$ (PBSCFO) have been investigated [17-22]. The researcher proposed BSCF as a suitable cathode composition candidate for intermediate temperature with improved performance, and this perovskite has high-ion conductivity [19] and superior catalytic performance in oxygen reduction [21-23] and a reasonable material cost [3]. In addition, BSCF is famous for having good stability and compatibility with electrolyte materials under fuel cell operating conditions such as BZCY, SDC, GDC, LSGM, YSZ and many more [24]. However, BSCF experiences chemical instability [25], thus decreasing the electrochemical performance [26], thus decreasing oxygen ion production. Moreover, the BSCF degrades over time because of the phase change from cubic to hexagonal phase, where it negatively affects cell performance [27]. Furthermore, BCSF has a high thermal expansion coefficient (TEC), which reflects to its poor incompatibility with the electrolyte and cathode interfaces [28].

A connection has been discovered on the BSCF cubic perovskite phase decomposition with the Co ion oxidation condition caused by oxygen nonstoichiometric (δ) change. Therefore, manipulating Co's oxidation state can sustain the cubic perovskite phase of BSCF [29]. The previous study proposed that the formation of oxygen vacancies promotes

perovskite phase stabilization [30]. Moreover, substituting higher valence cations for the B-site cation can enhance cell performance [29]. This substitution also can improve BSCF oxygen fluxes [31]. The elements of multivalent B-sites are selected for their superior ability to perform redox reactions in response to oxygen partial pressure during the SOFC operation [32]. Substitution of higher or lower valence cations on the B-site (Co / Fe) with $Ag^{1+,}$ Zn^{2+}, Sc^{3+}, Y^{3+}, Ti^{4+}, Nb^{5+}, Mo^{6+} and W^{6+} can help in stabilizing BSCF's cubic crystal structure and lowering thermal expansion coefficients [33-49].

In this short review, recent studies on transition metal element doping with BSCF-based cathode cathodes are reviewed and discussed regarding the effect of doping material on cathode cell performance. Possible cathode material for IT-SOFC can be developed and discovered following this review. The doping material emphasized in this review is Niobium (Nb), which is currently receiving significant attention [39], and Zinc (Zn), which is being continuously researched and provides an excellent attribute to the increase of oxygen flux [34]. The review work will cover the results and discussions on the chemical, physical, thermal and electrochemical properties achieved by previous research. The outcome between these two doping elements will be summarised.

Niobium-doping characteristic

The transformation of the perovskite structure from cubic to hexagonal phase is an inherent characteristic of BSCF-based materials that may be unavoidable at intermediate operating temperatures of SOFC. This scenario is caused by the slow cubic phase decomposition in Co, while the Ba side is enriched with hexagonal phase, resulting in a cubic phase deficient in Co and Ba. This phenomenon also decreases cell performance [26]. According to Egorova *et al.* (2015), partially substituted Niobium (Nb^{5+}) into the B-side (Co and Fe) can aid in the solution of the phase stability of BSCF-based materials at IT-SOFC.

The difference in interatomic distance in cubic and hexagonal perovskite structures shows a stabilization influence of Nb doping with BSCF perovskite structure. In the hexagonal structure, the interatomic distance of Co and Fe ions with the oxygen ions (Co—O and Fe—O) is lesser than that in the cubic structure [41]. According to the law of change neutrality, a reduction of valence cations on the B-site element can occur when Nb^{5+} is substituted into Co atoms in the BSCF system, and it can decrease the oxygen vacancy concentration [26]. When the oxidation state of the B-site element is reduced, the ionic radius will increase, thus increasing the chain length [41]. By substituting Co and Fe with Nb, the B-site cations are likely to adopt a cubic form with a greater distance of B-cations [26].

In addition, Nb^{5+} added to the Co and Fe atoms can reduce the valence in the B-site elements of the BSCF structure. Thus decreasing the oxygen vacancy content, where it can be addressed by changing the interatomic length between Co and Fe ions with oxygen ions and modifying the number of coordination and B-cation environment [26]. Wang *et al.* (2014) found a significant enhancement in the BSCF-based cathodes chemical stability under intense oxidation conditions after substituting Nb into B-site cations. The previous study findings will be reviewed and discussed in terms of how much Nb may increase the performance of the BSCF-based cathode.

Results and discussion on Nb-doping properties. In terms of chemical properties analysis, the testing involved was X-ray diffraction (XRD). Huang *et al.* (2020) reported that material depreciation could occur between the interface reaction of cathode and electrolyte, which should be avoided in the actual implementation of IT-SOFC. A phase identification analysis was done to examine the chemical compatibility of the composite cathode with the electrolyte. Figure 1(a) shows the phase diffraction pattern for BSCF, BSCFNb0.05, BSCFNb0.1, SDC and BSCFNb0.05-SDC samples. The graph indicates that BSCFNbx possesses a perovskite structure without an impurity phase. It is also verified that BSCFNbx is well-suited with the SDC as electrolyte material. Figure 1(b) shows the enlargement view of the XRD pattern at 2θ = 31.7°. As the Nb content increases, the diffraction peak shifts to the low-angle direction [38].

The lattice parameter was also calculated to determine the condition of the doping material in the BSCF-based cathode. The results show that with a higher level of Nb^{5+} doping, the cubic structure's lattice parameter expanded from 3.9851 Å to 3.9895 Å, where it is approximately equal to the lattice parameter of BSCF that reported in the previous study (3.9759 Å). Hence, cell volume increased, indicating that Nb^{5+} has a higher ionic radius than of 0.64 Å than Co^{4+} (0.53 Å) or Co^{3+} (0.61 Å) [38]. These occurrences can be ascribed to Nb's having a larger ionic radius than Co.

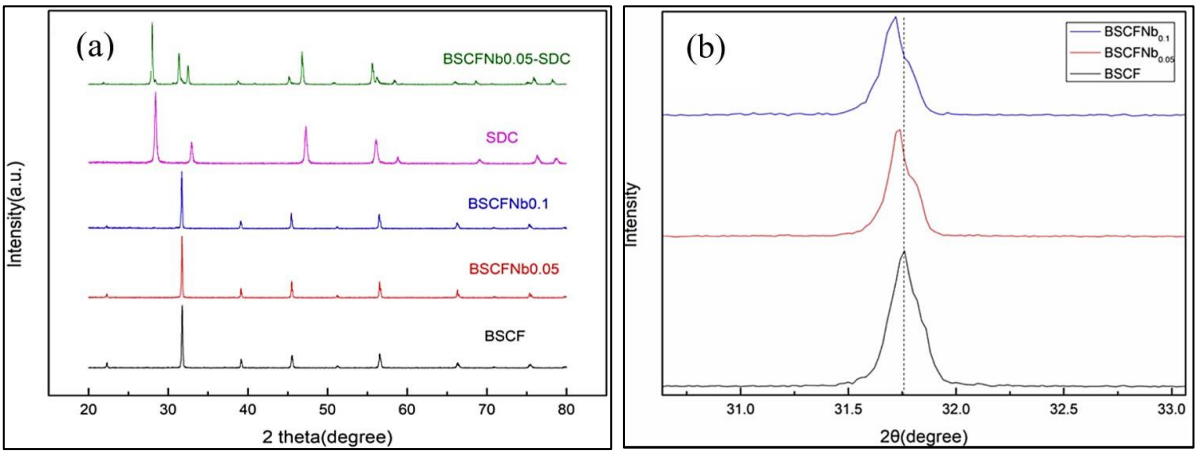

Figure 1. (a) The XRD pattern of BSCF, BSCFNb0.05, BSCFNb0.1, SDC and BSCFNb0.05-SDC composite powder after 3 hours of calcination at 1000 °C and (b) Magnified image (2θ = 31.7°) of XRD pattern for BSCF, BSCFNb0.05 and BSCFNb0.1 [38].

Figure 2(a) exhibits the SEM micrograph of cross-sectional view for a single-cell structure (NiO-BZCY|SDC|BSCFNb0.05-SDC). The cathode layer was firm merges with the electrolyte layer with no detected abnormalities, fractures, or delamination. The SEM image morphology result shows that the BSCFNb0.05-SDC sample is completely well-matched with the electrolyte. Figure 2(b) shows the surface morphology of SDC electrolyte, which displays a densely packed structure free of pores and cracks. Figure 2(c) shows the cross-sectional view of the BSCFNb0.05 cathode. The cathodes have an open pore structure that can improve and offer a good path for oxygen transport and a productive site for the ORR process [38, 42]. To prove that Nb-doping can obtain a fine structural condition with a BSCF-based cathode, Li *et al.* (2016) reported that the BSCFN|LSGM composite cathode is securely attached and shows no delamination signs. Figure 3 shows the dense LSGM

electrolyte and porous BSCFN composite cathode. It is indicated that the Nb doping shows good compatibility in physical properties toward BSCF-based cathode material.

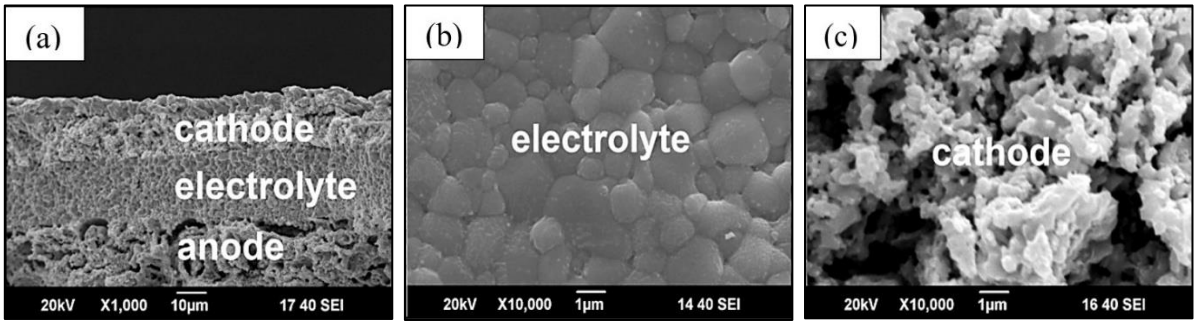

Figure 2. SEM image of (a) BSCFNb0.05 single cell structure in cross-sectional view, (b) SDS electrolyte surface morphology and (c) BSCFNb0.05 cathode in cross-sectional view [38].

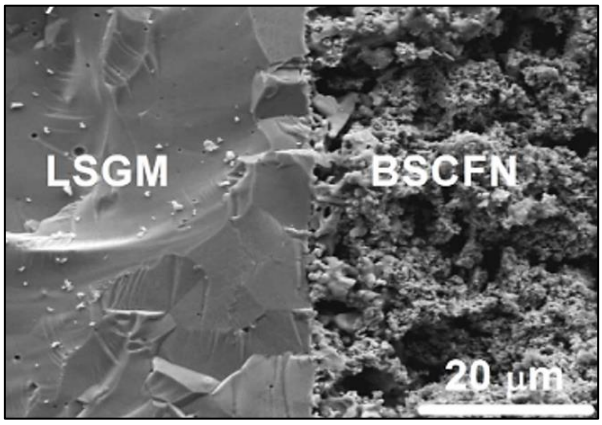

Figure 3. cross-sectional SEM morphology of BSCFN|LGSM composite cathode [29].

Furthermore, matching thermal expansion coefficient (TEC) values result in a superior electrolyte-electrode combination, which improves electrochemical performance and stability [38]. Yang et al. (2020) reported that in SOFC operation, the electrode materials must have specified mixed oxygen ion-electron hybrid conductivity, a lower interfacial polarisation, and a thermal expansion coefficient compatible with the electrolyte material. Figure 4 illustrates the curves of thermal expansion coefficients of BSCFNbx against temperature. The average of TEC values is displayed in Table 1.

From the observation, the average TEC values seem to decline as the amount of Nb^{5+} in the sample becomes greater in concentration. The binding energy of ions in the perovskite lattice is inversely associated to the TEC. When Nb^{5+} is doped, the B-O bonds are strengthened, and the TEC drops as a result [38]. As can be seen, all curves exhibit a shift in slope between 500 to 600 °C owing to the thermal decomposition of lattice oxygen [38, 46]. Additionally, the absence of lattice oxygen also decreasing the valence state of Co/Fe ions and weakens the bond between B and O. Therefore, the increasing lattice oxygen with rising temperature would improve the TEC values of BSCFNbx materials [38].

Table 1. The average of TEC values of BSCFNbx (x = 0, 0.05, 0.1) [38].

Material	The average of TEC values
BSCF	21.74 x 10^{-6} K^{-1}
BSCFNb0.05	19.67 x 10^{-6} K^{-1}
BSCFNb0.1	18.74 x 10^{-6} K^{-1}

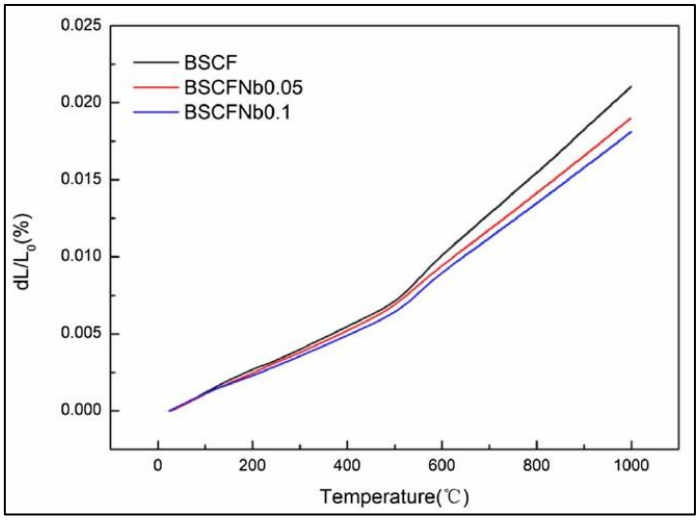

Figure 4. The TEC curves of BSCFNbx samples with temperature measured in air Atmosphere [38].

Figure 5 demonstrates the Ni-GDC|LDC|LSGM|BSCFN electrolyte supported single-cell impedance spectra at 600 °C, 650 °C, and 700 °C by an open-circuit voltage (OCV) state with using wet H^2 as fuel supply and atmospheric air supporting as the oxidant. Figure 5(b) shows the illustration graph of ohmic resistance (Ro) and total resistance (Rp) value against the operating temperature. Based on the graph image, the Ro and Rp value decreased substantially as the operating temperature increased. Figure 5(a) presents the fitted impedance spectra evaluated using the equivalent circuit in Figure 5(c). Where L represents the impedance and R: CPE indicates the resistance frequency range arcs as R_1: CPE at low range, R_2: CPE at the middle range, and R3:CPE at high range. As a finding, two small arcs can be seen in the high and middle frequency ranges connected with O_{2-} and change transport in the porous electrodes [23].

Meanwhile, large arcs that occurred at the low-frequency region are correlated with the cell reaction during gas migration. In addition, with the rise in running temperature, the resistance arcs at the high and medium frequency range decrease, suggesting that BSCFN benefits the O_{2-} transfer. Nevertheless, the resistance is more prevalent at the low-frequency range arc in these impedance spectra. Moreover, the microstructure of the porous electrodes could be optimized to improve bulk oxygen transport, which will indirectly improve cell efficiency [23]. It is because a porous state of morphology can help make a pathway for oxygen transport and increase the ORR activity of the sample.

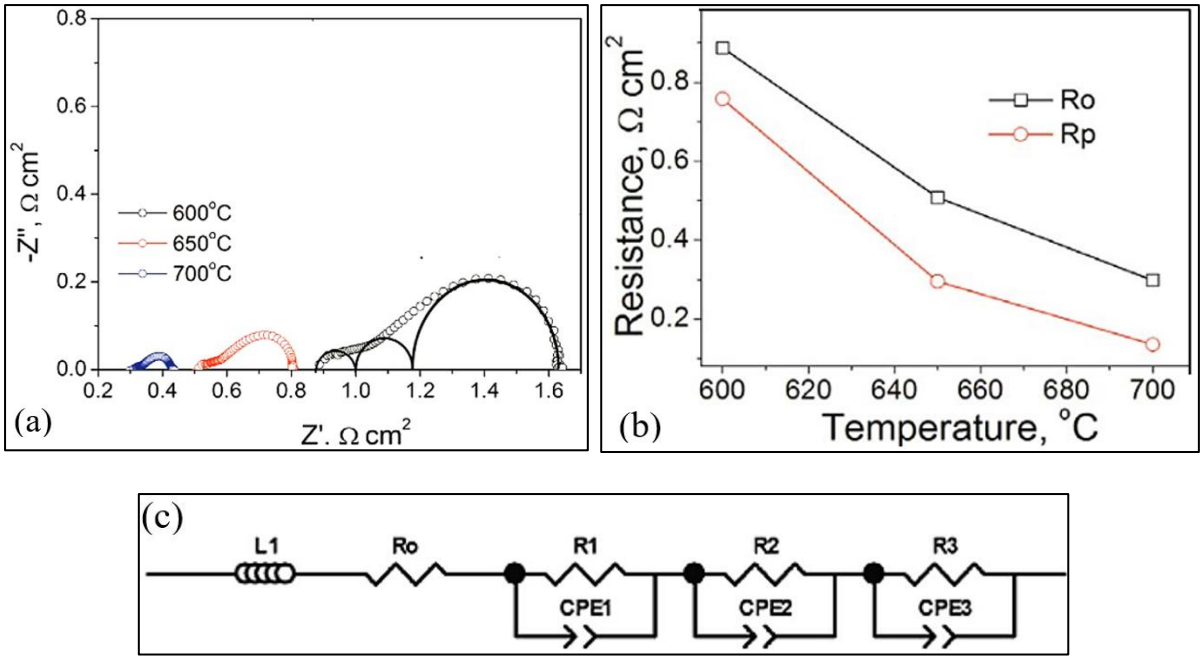

Figure 5. The Ni-GDC|LDC|LSGM|BSCFN single-cell impedance spectra, (a) Fitted impedance spectra, (b) Illustration of R_o and Rp plots against operational temperature and (c) equivalent circuit [23].

Figure 6 shows the cell voltage of electrolyte supported, Ni-GDC|LDC|LSGM|BSCFN, with a current controlled load of 0.6 Acm-2 for more than 100 hours at an operating temperature of 650 °C. The cell performs consistently based on the graph, and no signs of degradation have been detected. However, cell voltage slightly increased at a constant current load of 0.6 Acm-2 at 650 °C. This phenomenon occurred at the activation of the BSCFN cathode during the SOFC processes [23]. In addition, considering the stable chemical, physical and electrochemical properties of BSCFN perovskite cathodes with LSGM electrolyte, Nb can be combined with BSCF-based cathode and be a suitable cathode material for IT-SOFC.

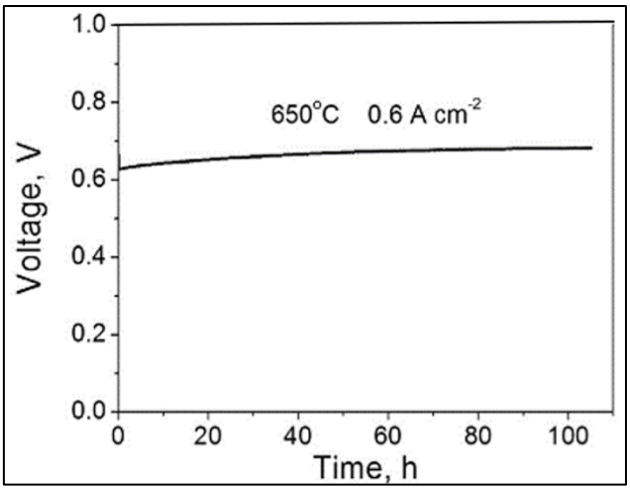

Figure 6. The Ni-GDC|LDC|LSGM|BSCFN electrolyte supported cell voltage [23].

Zinc-doping characteristic

Several groups have attempted to plan a strategy to improve BSCF performance at intermediate operating temperature. One of them is to identify the Cobalt-based materials that exhibit outstanding mixed ionic and electronic conductor (MIEC) properties to be the material candidates. A general MIEC perovskite such as BSCF has a chemical formula of $AA'BB'O_{3-\delta}$, which AA′ are typical alkaline earth metal ions and/or lanthanide metal ions. At BB′, the transition metal element usually is present [31]. $Ba_{0.5}Sr_{0.5}Co_{0.8}Fe_{0.2}O_{3-\delta}$ (BSCF) is a highly favourable compound for ceramic membranes because of its excellent oxygen permeability across a varied temperature region [19].

Nevertheless, cobalt-based materials experience several limitations; for instance, cobalt can quickly evaporate and be reduced, with a high thermal expansion coefficient [10]. A promising strategy has been discovered to improve BSCF-based cathode by substituting one cation in the B-site of BSCF [23-24, 32]. Several research papers have studied the substitution of transition element Niobium (Nb) with BSCF-based cathode. As previously stated, aside from Nb, Zinc has recently gained popularity as a desirable doping element.

Zinc (Zn) can maintain the chemical stability of BSCF under low oxygen partial pressures and changeable temperatures because of the Zn^{2+} constant oxidation state. Moreover, Zn^{2+} constant oxidation state can act as a barrier toward electronic conduction. This occurrence is referred to as the Zerner double exchange process. The electron conduction in perovskite material has a variable oxidation state that requires overlapping oxygen 2p orbital with the 3d of B-site metal [49]. Therefore, the optimum doping composition for Zn needs to be developed before it can be used as a cobalt substitute. Zeng *et al*. (2020) adopted minor Zinc doping, resulting in improved oxygen reduction reaction (ORR) catalytic activity and stability of BSCF as cathode material for SOFC. In this review, doping of Zinc on a BSCF-based cathode will be discussed and elaborated in terms of the improved impact of the doping element on the cathode composite.

Results and discussion on Zn-doping properties. A few tests were involved in analyzing the effect of the Zn-doping element on BSCF-based cathode. For the chemical properties, the result was determined via XRD. Park *et al.* (2011) stated that Zn-doping exhibits a well-crystallized XRD pattern, and all elements involved exist at their peaks with no secondary phase peaks appearing. Moreover, Zinc is certainly fit in the crystal structure at the B-site of perovskite and has positively responded when added to the cobalt. Table 2 displays the calculated lattice parameter of $Ba_{0.5}Sr_{0.5}Co_{0.2-x}Zn_xFe_{0.8}O_{3-\delta}$ powders, where x = 0-0.20. Based on the table, the lattice parameters were increased because of the lattice expansion, and the peak position moved slightly to the left. BSCF and BSZF have axis lengths of 3.9554 and 3.9778 Å, respectively. This finding was primarily credited to the higher ionic radius of doped Zn of 0.74 Å than Co by 0.53–0.65 Å and Fe by 0.55–0.78 Å [49]. This situation agreed that Zn has a larger ionic radius than Co and Fe also, it proves on the lattice expansion to some extent. Subsequently, as Zn doping content increased, so did the average a-axis length of cubic cells.

Table 2. Lattice parameter of Ba0.5Sr0.5Co0.2-xZnxFe0.8O3-δ powders, (x = 0-0.20) [49].

Material	Composition	Main peak position	Average a-axis (Å)	Cell volume ($Å^3$)
BSCF	$Ba_{0.5}Sr_{0.5}Co_{0.2}Fe_{0.8}$	31.973	3.9554	61.8830
BSZF	$Ba_{0.5}Sr_{0.5}Zn_{0.2}Co_{0.8}$	31.787	3.9778	62.9403
BSCZF05	$Ba_{0.5}Sr_{0.5}Co_{0.15}Zn_{0.05}Fe_{0.8}$	31.904	3.9626	62.2215
BSCZF10	$Ba_{0.5}Sr_{0.5}Co_{0.10}Zn_{0.10}Fe_{0.8}$	31.889	3.9654	62.3535
BSCZF15	$Ba_{0.5}Sr_{0.5}Co_{0.05}Zn_{0.15}Fe_{0.8}$	31.853	3.9696	62.5517

Zeng *et al.* (2020) studied BSCF-GDC and BSCFZ-GDC to assess the chemical compatibility of cathode material with the GDC buffer layer. A composite mixture of 50:50 ratio for each cathode composite was calcined for 6 hours at 1050 °C under ambient air. The composite powder was then subjected to XRD examination. Based on Figure 7, the XRD result indicates that each phase of BSCF, BSCFZ and GDC appear at peaks without the formation of impurities. Therefore, the materials have good chemical compatibility with one another even when under an operating temperature of above 700 °C [34].

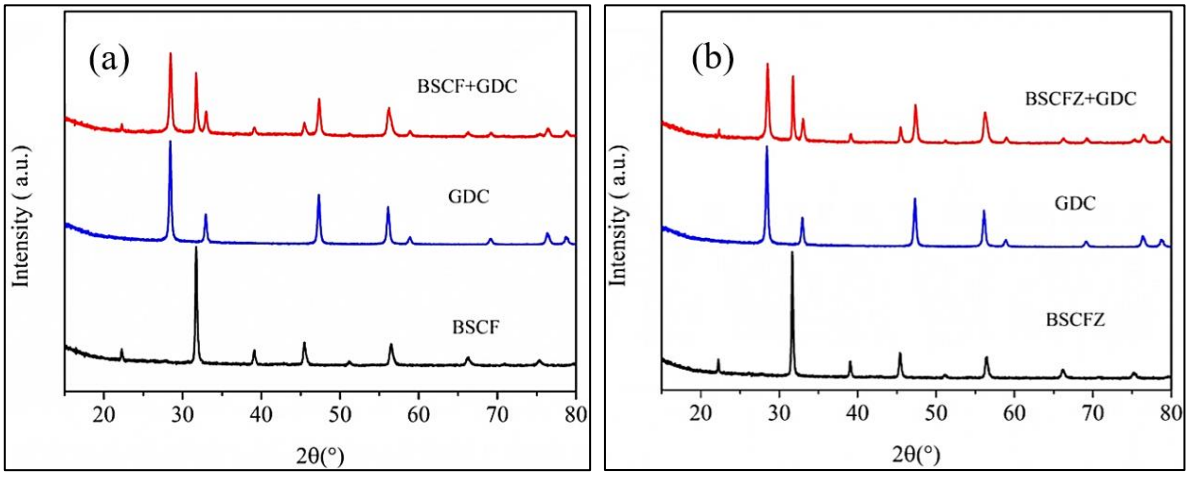

Figure 7. The patterns of XRD for (a) BSCF, GDC and BSCF+GDC powder, (b) BSCFZ, GDC and BSCFZ+GDC composite powder fired in air for 6 hours at 1050 °C [34].

Figure 8 displays the cross-sectional view of the BSCF, BSZF and BSCZF05 cathode layer [49]. Both samples were subjected to different sintering temperatures. All samples fired at 950 °C display an open structure for gas diffusions [50-51]. Once the temperature increased to 1000 °C, the BSCF cathode developed a denser layer with no detection of pores, while BSZF and BSCZF05 cathode maintained their open-pore structure. As the sintering temperature rises, the open-pore structure benefits gas diffusion and is necessary for oxygen transport [50-52]. Cobalt-based composites experience high thermal expansion. As reported by Park (2011), Zinc's constant oxidation state can undergo structural changes, such as agglomeration. Hence, the presence of Zinc in cobalt-containing perovskite can suppress the side effect of the sintering process. Zeng *et al.* (2020) also reported that the GDC buffer layer and porous BSCFZ cathode are nicely joined without delamination. The porous structure of

the cathode would improve cell performance by facilitating oxygen transportation and increasing active sites for ORR [34].

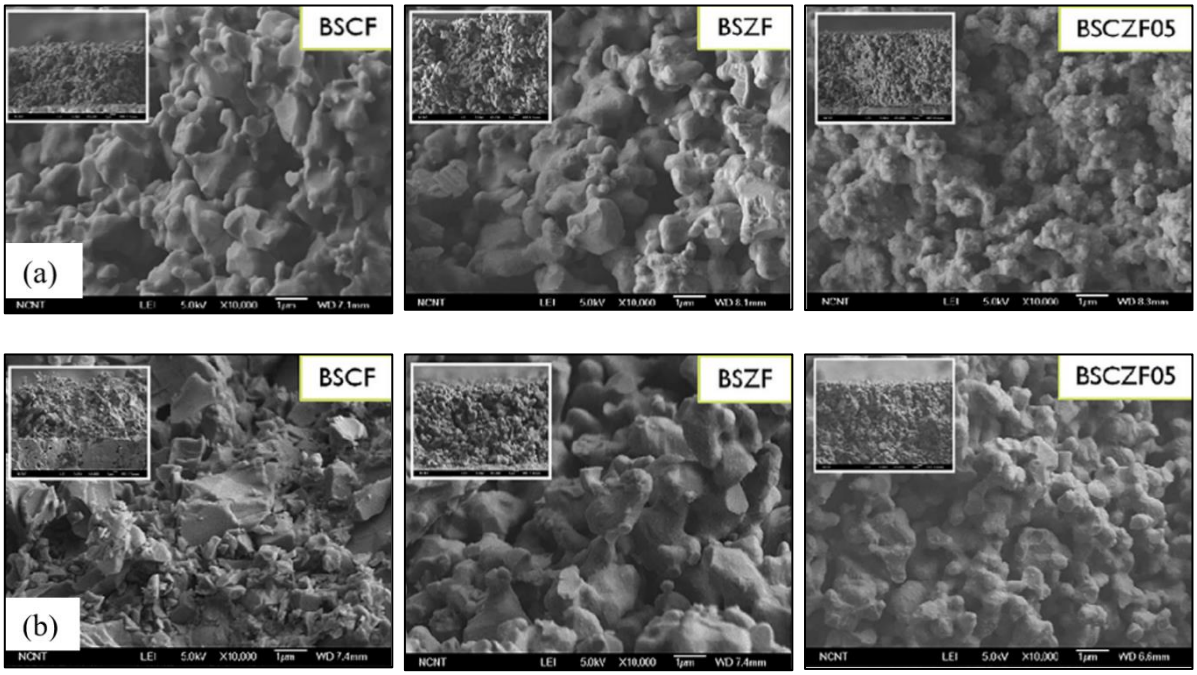

Figure 8. SEM images of BSCF, BSZF and BSCZF05 cathode layer after sintering process at (a) 950 and (b) 1,000 °C [34].

Long-term operation of SOFCs is jeopardised by mismatch in thermal expansion behaviour between the electrode and electrolyte, which may result in cracking and delamination of the components, as well as a reduction in overall cell performance. It has been claimed that the TEC value for a Co-rich perovskite material regularly reaches 20-30 x 10^{-6} K^{-1} [53]. However, Park (2011) reported that Zinc's constant oxidation state may be able to prevent structural changes such as thermal expansion from occurring. Thus, zinc doping seems to inhibit the sintering of cobalt-containing perovskites in the cathode layer. Figure 9 illustrates the H_2-TPR result curves for BSCF and BSCZF05 sintered at 950 °C and 1000 °C. Refer to the graph, the first peak corresponds to a reduction of Co^{4+} to Co^{3+} [50]. When comparing the intensity of this peak at 950 °C to that of the peak at 1000 °C, it was discovered that when the sintering temperature ascended, BSCF's first peak's intensity declined substantially, and BSCZF05's intensity dropped just slightly. The reduced stability of Co^{4+} ions has been shown to result in a greater oxygen conductivity at low temperatures [50].

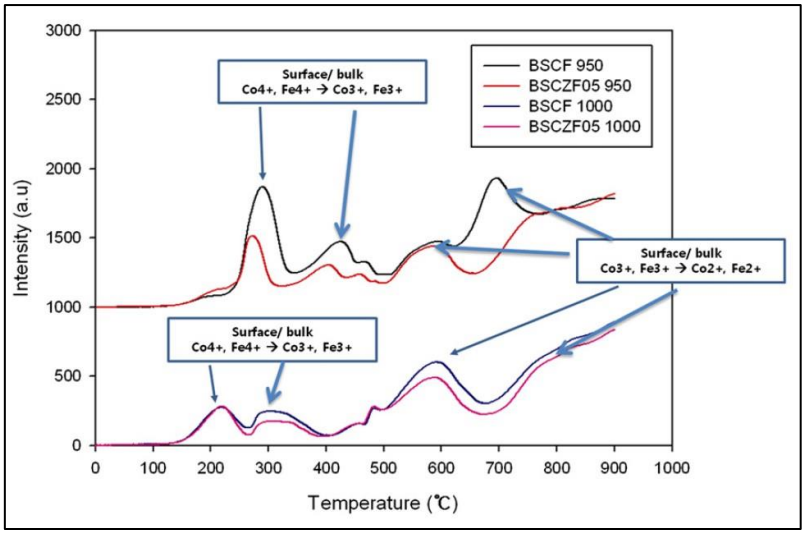

Figure 9. H_2-TPR result curves for BSCF and BSCZF05 sintered at 950 and 1000 °C [50].

Anode-supported single cells were examined with the electrochemical impedance spectra (EIS) testing at temperatures 750, 700, and 650 °C to determine the performance of the BSCF cathode composite under the influence of the Zn-doping element. Figure 10(a) shows the equivalent circuit used to fit the Nyquist plot and obtain the impedance results [34]. Figure 10(b) shows the polarization resistance (R_p) value of BSCF and BSCFZ cathodes against the operating temperature. The polarisation resistance (R_p) in a single cell is mainly ascribed as cathode polarisation because, generally, anode polarization is considered minor [34]. Figure 10(b) shows that the R_p value for both cells decrease with the operating temperature increase. The Zn-doping (BSCFZ) composite cathode remarkably decreased R_p, indicating that the O^{2-} transfer, oxygen reduction and diffusion processes were elevated because, at the BSCFZ cathode, there is increasing in oxygen vacancy concentration and ORR activity.

Figure 11 displays the single cells impedance spectra results for 11(a) BSCF and 11(b) BSCFZ cathode at operating temperatures of 650, 700 and 750 °C. The curve represented in the impedance spectra is R_1 and R_2, where R_1 (high-frequency arc) is the charge transfer resistance associated with oxygen-ion (O^{2-}) and the charge transfer at the electrode and electrode/electrolyte interface. R_2 (low-frequency arc) is the resistance of the oxygen surface exchange and diffusion process associated with the concentration of oxygen vacancy and the microstructure of the electrode [34, 51]. Based on Figure 11(b), the R_1 curve is reduced with increasing temperature, showing that Zn-doping improved O^{2-} transfer in BSCF-based cathodes. Meanwhile, the R_2 curve dominates in this fitted impedance spectra result. Therefore, the properties of single cells can be improved by optimizing the microstructure of electrodes to allow mass transport cation [34]. This supports the morphology theory that a porous state in the cell sample can help the ORR catalytic activity.

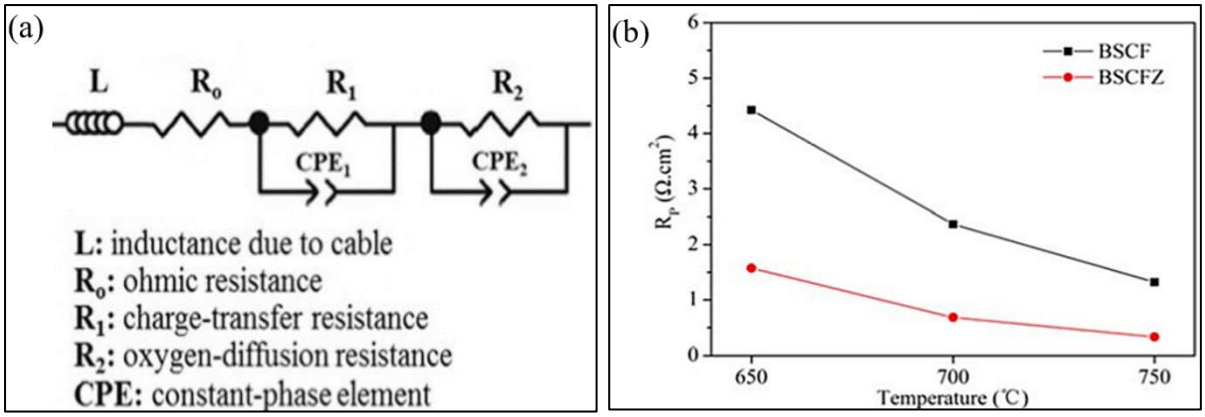

Figure 10. (a) Equivalent circuit and (b) summarized Rp value for BSCF and BSCFZ [34].

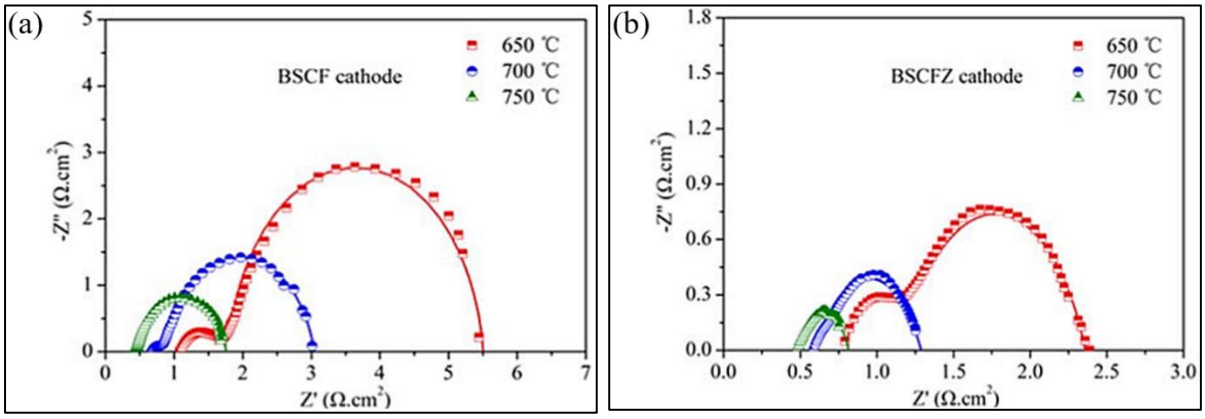

Figure 11. Single cells impedance spectra results at operational temperature 650, 700 and 750 °C for (a) BSCF and (b) BSCFZ cathodes [34].

A single cell of BSCF and BSCFZ cathodes was tested for stability for 140 hours at temperature 750 °C with 0.7 V of voltage level. Figure 12 depicts the effect of run time on the current density of a single cell. The results show that the cell current density of the BSCFZ cathode was almost barely changed, except for a modest increment in the first hundreds of hours because of the cathode activation process with increased temperature [34, 50]. The cell with a BSCF cathode was observed, and the current density decreased at 750 °C after 140 hours. The result indicates that the cell has been improved, and BSCFZ cubic perovskite structure has improved phase stability [34].

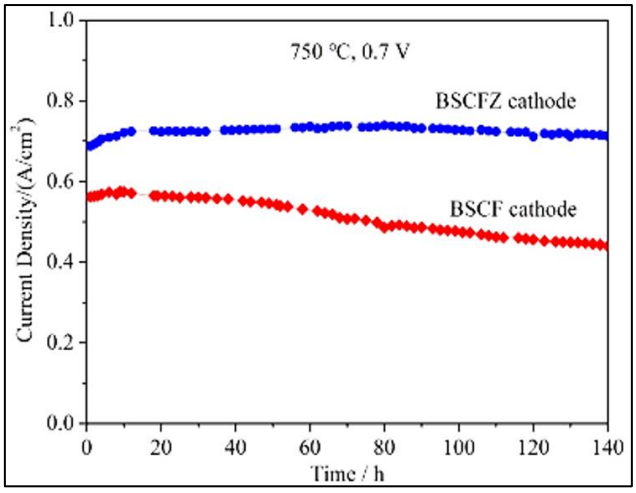

Figure 12. Trend of current density for single cells with BSCF and BSCFZ cathode at 750 °C [34].

Based on the investigation by Park *et al.* (2011), the BSCZF05 sample is more dominant in decreasing interfacial resistance with increasing sintering temperature. This situation is related to the strong adhesion between the electrode and electrolyte particle, thus reducing the interfacial resistance. Figure 13 displays the BSCZF05-SDC 30 wt% composite cathode impedance spectra that are sintered at 1000 °C. At operating temperatures of 700, 650 and 600 °C, the R_p values recorded were 0.09, 0.32 and 0.44 Ωcm^2, respectively. These recorded values surpass other composite cathodes such as LSCF-GDC with Rp value 0.6 Ωcm^2 at 590 °C [50].

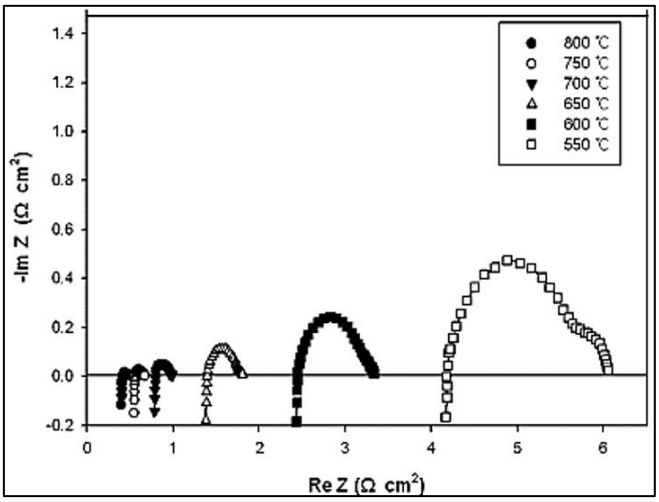

Figure 13. The BSCZF05-SDC 30 wt% composite cathode impedance spectra plot at temperature 550 °C – 800 °C [50].

Conclusion

This paper reviews recent results on substituting niobium (Nb) and Zinc (Zn) as doping materials for BSCF-based cathode. The influence of transition element substitution on the B-site of BSCF-based cathode material for IT-SOFC was discussed. The results showed by Nb and Zn doping with BSCF-based cathode indicated that both outcomes improved the physical, chemical, thermal and electrochemical properties of the cathode cell. It also helps balance the chemical stability and increase the ORR catalytic activity.

In addition, this work concludes that there are still many works that can be done to investigate how much doping from transition metal element group can contribute as the catalyst on BSCF-based cathode material. The theory on substitution elements at the B-site of BSCF-based cathode clearly shows an improvement in cell performance properties. Extensive research is still required to investigate the contribution of transition metal element doping to the BSCF-based cathode or other perovskite materials.

The results of this work may help determine the optimum parameter for IT-SOFC and provide beneficial results on the material properties, such as improvement on the conductivity, catalytic activity, chemical, thermal and physical properties. Furthermore, the development of cathode material for IT-SOFC can enable the limitation faced by the SOFC at high temperatures and improve SOFC commercialization. The results of this review can be beneficial and informative to accomplish these goals.

Acknowledgements

The authors would like to express their gratitude to the Malaysian Ministry of Higher Education (MOHE) for supporting this research through Fundamental Research Grant Scheme (FRGS/1/2020/TK0/UTHM/02/15) and partially funded by Universiti Tun Hussein Onn Malaysia (UTHM) under Postgraduate Research Grant (GPPS H692).

Author Contributions

All authors contributed toward data analysis, drafting and critically revising the paper and agree to be accountable for all aspects of the work.

Disclosure of Conflict of Interest

The authors have no disclosures to declare.

Compliance with Ethical Standards

The work is compliant with ethical standards.

References

[1] Wan, R. W. D., Arshad, A., Abu, B. M., Siti, K. K., Joseph, K. I. S., Nurfarizal, R., Zulfadli, D., Umi, A. H., Nitia, S. & Mohd, I. A. (2017). *The Blueprint for Fuel Cell Industries in Malaysia*. 1st edition (Academy of Science Malaysia) pp. 77.

[2] Leonardo, G. & Fabio, L. (2013). Fuel cells: Technologies and applications. *The Open Fuel Cells J*. 6 1-20.

[3] Wei, Z., Ran, R. & Zongping, S. (2009). Progress in understanding and development of $Ba_{0.5}Sr_{0.5}Co_{0.8}Fe_{0.2}O_{3-\delta}$-based cathodes for intermediate-temperature solid-oxide fuel cells: A review. *J. Power Sources*. 192 231–246.

[4] Jeffrey, W. F., Rob, H., Xianguo, L., David, P. W. & Jiujun, Z. (2009). *Solid oxide fuel cells: Materials properties and performance*. 1st edition (CRC Press) pp. 295.

[5] Liangdong, F., Bin, Z., Pei-Chen, S. & Chuanxin, H. (2018). Nanomaterials and technologies for low temperature solid oxide fuel cells: Recent advances, challenges and opportunities. *Nano Energy*. 45 148–176.

[6] Linda, A., Muhammad, S. A. B., Sufizar, A., Andanastuti, M. & Hamimah, A. R. (2015). Influence of Ag on Chemical and Thermal Compatibility of LSCF-SDCC for LT-SOFC. *Appl. Mech. Mater*. 773 445–449.

[7] Takaya, O., Mizutomo, T. & Yuya, K. (2018). Comprehensive analysis of trends and emerging technologies in all types of fuel cells based on a computational method. *Sustainability*. 10 458.

[8] Qidong, X., Zengjia, G., Lingchao, X., Qijiao, H., Zheng, Li., Idris, T. B., Keqing, Z. & Meng, N. (2022). A comprehensive review of solid oxide fuel cells operating on various promising alternatives fuels. *Energy Convers. Manag.* 253 115175.

[9] Vanja, S., Arianna, B., Linda, B., Robert, S., Gernot, P., Christoph, H. & Andrés, A. C. (2019). Applicability of the SOFC technology for coupling with biomass-gasifier systems: Short- and long-term experimental study on SOFC performance and degradation behaviour. *Appl. Energy*. 256 113904.

[10] Abdalla, M. A., Shahzad, H., Atia, T. A., Pg, M. I. P., Feroza, B., Sten, G. E. & Abul, K. A. Nanomaterials for solid oxide fuel cells: A review. (2018). *Renew. Sustain. Energy Rev.* 82 353–368.

[11] Jeong, W. S., Dohyun, G., Seung, H. K., Sungje, L. & Jihwan, A. (2019). Review on process-microstructure-performance relationship in ALD-engineered SOFCs. *J. Phys. Energy.* 1 042002.

[12] Irina, P., Mirela, D. & Silvin, L. B. (2020). *Fuel Cells: Alternative Energy Sources for Stationary, Mobile and Automotive Applications.* Ebook edition (IntechOpen) pp. 272.

[13] Jih-Sheng, L. & Michael, W. E. (2017). Fuel Cell Power Systems and Applications. In: *Proceeding of the IEEE,* vol. 105. pp. 2166-2189.

[14] Xi, X., Huiqiang, W., Marco, F., Xianfen, W., Lei, B. & Enrico, T. (2019). Tailoring cations in a perovskite cathode for proton-conducting solid oxide fuel cells with high performance. *J. Mater. Chem. A.* 7(36) 20624–20632.

[15] Quan, Y., Dong, T., Rui L., Haodong, W., Yonghong, C., Yanzhi, D., Xiaoyong, L. & Bin, L. (2021). Exploiting rare-earth-abundant layered perovskite cathodes of $LnBa_{0.5}Sr_{0.5}Co_{1.5}Fe_{0.5}O_{5+\delta}$ (Ln=La and Nd) for SOFCs. *Int. J. Hydrog. Energy*. 46 5630-5641.

[16] Peng, Q., Jin, L., Lichao, J., Bo, C., Jian, P., Jian, L. & Fanglin, C. (2019). $LaCoO_{3-\delta}$ coated $Ba_{0.5}Sr_{0.5}Co_{0.8}Fe_{0.2}O_{3-\delta}$ cathode for intermediate temperature solid oxide fuel cells. *Electrochim. Acta*. 319 981–989.

[17] Sudhanshu, D. (2020). Solid oxide fuel cell: Materials for anode, cathode and electrolyte. *Int. J. Hydrog. Energy*. 45 23988–24013.

[18] San, P. J. (2019). Development of lanthanum strontium cobalt ferrite perovskite electrodes of solid oxide fuel cells – A review. *Int. J. Hydrog. Energy*. 44 7448–7493.

[19] Muhammet, S. T., Mahdi, D., Guttorm, E. S. & Mamoun, M. (2010). Synthesis of nanostructured BSCF by oxalate co-precipitation – As potential cathode material for solid oxide fuels cells. *Int. J. Hydrog. Energy*. 35 9448–9454.

[20] Catarina, M., Antonio, F. & Diogo, M. F. S. (2021). Towards the commercialization of solid oxide fuel cells: Recent advances in materials and integration strategies. *Fuels*. 2 393-419.

[21] Anisah, S. H., Nafisah, O. & Abdul, M. M. J. (2020). Microstructural investigation of BSCF-based cathode material for enhanced oxygen reduction reaction performance and electrode stability. *Ceram. Int.* 46 23262–23265.

[22] Huan, L. & Zhe, L. (2020). A highly stable cobalt-free $LaBa_{0.5}Sr_{0.5}Fe_2O_{6-\delta}$ oxide as a high-performance cathode material for solid oxide fuel cells. *Int. J. Hydrog. Energy*. 45 19831-19839.

[23] Jiao, L., Chenghao, Y. & Meilin, L. (2016). High performance intermediate temperature solid oxide fuel cells with $Ba_{0.5}Sr_{0.5}Co_{0.8}Fe_{0.1}Nb_{0.1}O_{3-\delta}$ as cathode. *Ceram. Int.* 42(16) 19397–19401.

[24] Saddam, H. & Li, Y. (2020). Review of solid oxide fuel cell materials: cathode, anode and electrolyte. *Energy Trans.* 4 113-126.

[25] Prasopchokkul, P., Seeharaj, P. & Kim-Lohsoontorn, P. (2020). $Ba_{0\cdot5}Sr_{0\cdot5}(Co_{0\cdot8}Fe_{0.2})_{1-x}Ta_xO_{3-\delta}$ perovskite anode in solid oxide electrolysis cell for hydrogen production from high-temperature steam electrolysis. *Int. J. Hydrog. Energy*. 45(10) 7023-7036.

[26] Egorova, Y. V., Scherb, T., G., Bouwmeester, H. J. M. & Filatova, E. O. (2015). Soft X-ray absorption spectroscopy study of $(Ba_{0.5}Sr_{0.5})$ $(Co_{0.8}Fe_{0.2})_{1-x}Nb_xO_{3-\delta}$ with different content of Nb (5%-20%). *J. Alloys Compd.* 650 848–852.

[27] Lucia, D. S., Javier, Z., Jose, M. P., Enrique, R. L. & David, M. (2020). Nanostructured $BaCo_{0.4}Fe_{0.4}Zr_{0.1}Y_{0.1}O_{3-\delta}$ Cathodes with Different Microstructural Architectures. *Nanomaterials*. 10 1055.

[28] Stephan, J. S. (2001). Recent advances in perovskite-type materials for solid oxide fuel cell cathodes. *Int. J. Inorg. Mater*. 3 113–121.

[29] Fang, W., Takashi, N., Keiji, Y., Junichiro, M. & Koji, A. (2014). Effect of Nb doping on the chemical stability of BSCF-based solid solutions. *Solid State Ion.* 262 719–723.

[30] Junxing, Z., Ximu, L., Zhenbao, Z., Xiaomin, X., Yubo, C., Yufei, S., Jie, D., Guangming, Y., Ran, R., Wei, Z. & Zongping, S. (2020). A new highly active and CO_2-stable perovskite-type cathode material for solid oxide fuel cells developed from A- and B-site cation synergy. *J. Power Sources*. 457 227995.

[31] Xiaozhen, Z., Julius, M., Shaomin, L. & Joao, C. D. D. C. (2017). Zinc-doped BSCF perovskite membranes for oxygen separation. *Sep. Purif. Technol.* 189 399–404.

[32] Paramvir, K. & Singh, K. (2020). Review of perovskite-structure related cathode materials for solid oxide fuel cells. *Ceram. Int.* 46 5521–5535.

[33] Umira, A. Y., Kang, H. T. & Hamimah, A. R. (2019). Structure and Thermal Behaviour of BSCF-SDC-Ag Composite Cathode for Solid Oxide Fuel Cell. *Int. J. Eng. Adv. Tech.* 9(2) 1582–1585.

[34] Qiannan, Z, Xiaozhen, Z., Wei, W., Dandan, Z., Yuhua, J., Xiaojian, Z. & Bin, L. (2020). A Zn-doped $Ba_{0.5}Sr_{0.5}Co_{0.8}Fe_{0.2}O_{3-\delta}$ perovskite cathode with enhanced ORR catalytic activity for SOFCs. *Catalysts*. 10(2) 235.

[35] Daniel, D. A., Douglas, F. S., Alysson, M. A. S., Daniela, V., Eduardo, H. M. N., Julius, M., Joao, C. D. D. C. & Wander, L. V. (2017). Carbonation passivation layer of scandium loaded BSCF perovskite. *Ceram. Int.* 43 15179–15184.

[36] Laura, A., Heiki, S., Matthias, M., Julian, S., Florian, W., Dagmar, G. & Ellen, I. (2018). Improved Phase Stability and CO_2 Poisoning Robustness of Y-doped $Ba_{0.5}Sr_{0.5}Co_{0.8}Fe_{0.2}O_{3-\delta}$ SOFC Cathodes at Intermediate Temperatures. *ACS Appl. Energy Mater.* 1(3) 1316-1327.

[37] Hui, L., Jinna, Z., Qiuping, Z. & Jianzhou, G. (2020). Novel $Ba_{0.15}Sr_{0.85}M_{0.15}Fe_{0.85}O_{3-\delta}$ (M = Fe, Co, Al, Ti) perovskite oxides for oxygen enrichment: Structural, electrical, and oxygen sorption/desorption properties. *Mater. Sci. Eng.* 262 114686.

[38] Yuwen, H., Jinwen, D., Yunpeng, X., Lina, M., Kang, L. & Qingping, Z. (2020). $Ba_{0.5}Sr_{0.5}Co_{0.8-x}Fe_{0.2}Nb_xO_{3-\delta}$ ($x \leq 0.1$) as cathode materials for intermediate temperature solid oxide fuel cells with an electron-blocking interlayer. *Ceram. Int.* 46 10215-10223.

[39] Wenyun, L., Hongning, K., Xianfen, W., Lei, B. & Zhao, X. S. (2019). Improving the performance of the $Ba_{0.5}Sr_{0.5}Co_{0.2}Fe_{0.8}O_{3-\delta}$ cathode for proton-conducting SOFCs by microwave sintering. *Ceram. Int.* 45 20994-20998.

[40] Junxing, Z., Zhenbao, Z., Yubo, C., Xiaomin, X., Chuan, Z., Guangming, Y., Wei, Z. & Zongping, S. (2018). Materials design for ceramic oxygen permeation membranes: Single perovskite vs. single/double perovskite composite, a case study of tungsten-doped barium strontium cobalt ferrite. *J. Membr. Sci.* 566 278–287.

[41] Yunfei, C., Hailei, Z., Deqiang, T., Fushen, L., Xionggang, L. & Weizhing, D. (2008). Investigation of Ba fully occupied A-site $BaCo_{0.7}Fe_{0.3-x}Nb_xO_{3-\delta}$ perovskite stabilized by low concentration of Nb for oxygen permeation membrane. *J. Membr. Sci.* 322 484–490.

[42] Miaomiao, G., Qiang, L., Juntao, G., Liping, S., Lihua, H. & Hui, Z. (2020). Highly electrocatalytic active and durable Fe-based perovskite oxygen reduction electrode for solid oxide fuel cells. *J. Alloys Compd.* 858 158265.

[43] Shubnikovaa, E. V, Braginaa, O. A. & Nemudrya, A. P. (2018). Mixed conducting molybdenum doped BSCF materials. *J. Ind. Eng. Chem*. 59 242-250.

[44] Lei, B., Emiliana, F. & Enrico, T. (2012). Novel $Ba_{0.5}Sr_{0.5}(Co_{0.8}Fe_{0.2})_{1-x}Ti_xO_{3-\delta}$ (x=0, 0.05, and 0.1) cathode materials for proton-conducting solid oxide fuel cells. *Solid State Ion.* 214 1-5.

[45] Ye, L., Ran, R. & Zongping, S. (2010). Silver-modified $Ba_{0.5}Sr_{0.5}Co_{0.8}Fe_{0.2}O_{3-\delta}$ as cathodes for a proton conducting solid-oxide fuel cell. *Int. J. Hydrog. Energy.* 35 8281-8288.

[46] Fang, S.M., Yoo, C.Y. & Bouwmeester, H. J. M. (2011). Performance and stability of niobium-substituted $Ba_{0.5}Sr_{0.5}Co_{0.8}Fe_{0.2}O_{3-\delta}$ membranes. *Solid State Ion.* 195 1-6.

[47] Umira, A. Y., Kang, H. T., Hamimah, A. R., Nurul, A. B. & Jarot, R. (2020). Electrochemical performance of barium strontium cobalt ferrite -samarium doped ceria–argentum for low-temperature solid oxide fuel cells. *Mater. Sci. Forum*. 991 94-100.

[48] Doh, W. J., Chan, K., Hee, J. P., Ju, S. K., Sung, J. A., Dong, H. Y., Sooyeon, S., Kyeong, S. M. & Sang, M. L. (2016). High-performance perovskite $Ba_{0.5}Sr_{0.5}Co_{0.8}Fe_{0.1}O_{3-\delta}$ – $La_{0.6}Sr_{0.4}Co_{0.2}Fe_{0.8}O_{3-\delta}$ composite cathode. *Scr. Mater.* 113 59-62.

[49] Xue, Y., Ruoyu, L., Yang, Y., Guilin, W., Dong, T., Xiaoyong, L., Yanzhi, D., Yonghong, C. & Bin, L. (2020). Improving stability and electrochemical performance of $Ba_{0.5}Sr_{0.5}Co_{0.2}Fe_{0.8}O_{3-\delta}$ electrode for symmetrical solid oxide fuel cells by Mo doping. *J. Alloys Compd.* 831 154711.

[50] Jungdeok, P., Jing, Z., Heechul, Y., Guntae, K. & Jong, S. C. (2011). Electrochemical behavior of $Ba_{0.5}Sr_{0.5}Co_{0.2-x}Zn_xFe_{0.8}O_{3-\delta}$ (x = 0-0.2) perovskite oxides for the cathode of solid oxide fuel cells. *Int. J. Hydrog. Energy*. 36 6184-6193.

[51] Davide, C., Sabrina, P., Maria, P. C., Antonio, B., Francesca, D., Leonarda, F. L., Chiara, A. & Massimo, V. (2019). Distribution of Relaxation Times and Equivalent Circuits Analysis of $Ba_{0.5}Sr_{0.5}Co_{0.8}Fe_{0.2}O_{3-\delta}$. *Catalysts*. 9 441.

[52] Shuang, Z., Ning, T. & Ji, Y. (2020). Performance of $Ba_{0.5}Sr_{0.5}Co_{0.8}Fe_{0.2}O_{3-\delta}/Ce_{0.85}Sm_{0.15}O_{2-\delta}$–CuO as a cathode for intermediate temperature solid oxide fuel cells. *J. Alloys Compd.* 825 154013.

[53] Wenwen, Z., Lifang, Z., Kai, G., Xiong, Z., Junling, M., Haocong, W., Xiaojuan, L. & Jian, M. (2020). Effective promotion of oxygen reduction activity by rare earth doping in simple perovskite cathodes for intermediate-temperature solid oxide fuel cells. *J. Power Sources.* 446 227360.